Eur. J. Biochem. 44, 195—199 (1974)

Electron-Paramagnetic-Resonance Study of Manganese Ions Bound to Concanavalin A

Eberhard VON GOLDAMMER and Herbert ZORN

Lehrstuhl für Physik, Fachbereich Biologie, Universität Regensburg

(Received November 3, 1973/February 11, 1974)

The electron paramagnetic resonance (EPR) line shape of Mn^{2+} ions bound in crystallized concanavalin A has been analyzed at two microwave frequencies, 9 and 35 GHz. From a comparison between measured and simulated EPR-spectra, the correlation times for the process modulating the zero field splitting (zfs) interaction and the magntiude of the zfs-parameters have been determined. In the absence of Ca^{2+} ions a correlation time of 10 ps (at 4 °C), typical for the thermal motions of the diffusing transition metal ions, has been determined. In the presence of Ca^{2+} ions the Mn^{2+}-spectrum of concanavalin A reveals forbidden transitions ($\Delta m = \pm 1$), indicating that the mean life-time for the transition metal ions at the binding site S1 is increased ($\tau_{ass} \gtrsim 10$ ns) under the action of calcium ions bound at S2.

Concanavalin A is one of the four crystallizable globulins of the jack bean (*Canavalia ensiformis*) [1]. It is known by its hemagglutinating activity [1,2] and its ability of precipitating various polysaccharides, such as glycogen and yeast mannans [3]. Among its biological properties, concanavalin A also agglutinates leukemic cells and cells transformed by polyoma virus, simian virus 40, chemical carcinogens, and X-irradiation [4].

The protomeric unit of concanavalin A has a molecular weight of about 27000 [5]. In solution the protein consists of dimers at pH values less than 6 and of tetramers above pH 7 [5]. Each subunit has two binding sites for metal ions: a site (S1) for transition metal ions and a site (S2) specific for calcium ions. The protein only maintains its agglutinating ability if both sites are occupied [1,6]. It is lost after treatment with acid followed by neutralization, but on standing it returns completely, provided the acid has not been too concentrated [1] and the metal ions have been not removed by dialysis.

In order to understand the significance of the two metal ions supporting a particular protein structure, we have analysed the EPR-spectra of manganese in the presence and absence of calcium ions in crystallized concanavalin A.

MATERIALS AND METHODS

Concanavalin A was purchased by Boehringer Mannheim GmbH (Mannheim, Germany). A suspension of 250 mg in 10 ml of a 4 M NaCl solution was dialysed (Visking 20/32) against twice-distilled water and then diluted with twice-distilled water to a total volume of 25 ml. The protein was demetallized by addition of 1 M HCl to give a pH of 1.2, measured by a glass electrode. After standing for 1 h at 4 °C the solution was transferred into dialysis bags that had been treated with 1 mM EDTA and dialysed against three changes of 2 l of twice-distilled water [6]. $CaCl_2 \cdot 2\,H_2O$ and/or $MnCl_2 \cdot 4\,H_2O$ was added to 5-ml portions of the resulting solution. The cation concentration was chosen to be 20 mM. After standing for 2 h these solutions were dialysed against 0.05 M-Tris-HCl buffer pH = 7.4, containing 1 mM Ca^{2+} and/or Mn^{2+} ions. The protein crystallizes readily. The crystals were washed three times with twice-distilled water and were centrifuged into specially prepared liquid sample tubes (a capillary of about 2-cm length and 0.3-mm inner diameter was drawn from a 2-mm quartz tube). The water phase was collected and its relative manganese concentration referred to the corresponding volume of the protein in the sample tube was determined by EPR in a double cavity (*cf.* Fig. 1). The Mn^{2+} concentration in the bulk water phase was found to be about 10 times less than the Mn^{2+} concentration in the crystallized (centrifuged) protein phase. In Fig. 1 two EPR-spectra corresponding to the protein and the bulk water phase are presented.

All EPR-spectra were registered with a Varian-E9 100-kHz field modulation spectrometer at 9.5 GHz (X-band) and 35 GHz (Q-band). Sample temperatures were controlled with a Varian-E 4557 variable

Abbreviations. EPR, electron paramagnetic resonance; zfs, zero field splitting.

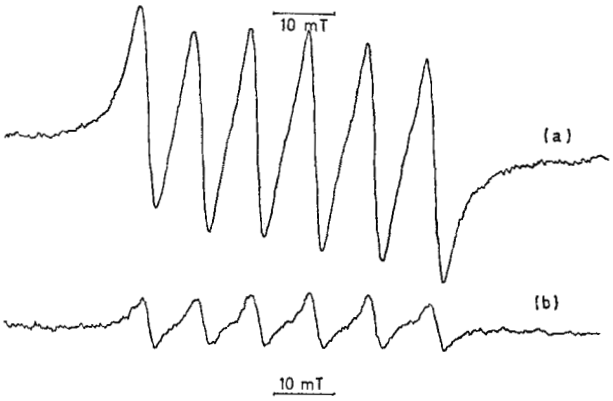

Fig. 1. *Mn^{2+}-EPR spectrum of centrifuged concanavalin A crystals (curve a) and the bulk water phase (curve b; amplified 1.6×) with equivalent sample volumes at room temperature*

temperature assembly and were measured with a chromel-alumel thermocouple inserted in the nitrogen stream. Its accuracy was ± 1 K and ± 3 K for the X-band and Q-band, respectively.

All calculations and spectra simulations were executed, as previously described [7], on a Siemens 4004 computer and an CIL 6011 off-line plotter.

THEORY

Generally it has been accepted that the relaxation mechanism determining the EPR line shape of manganese ions in the "high temperature" (*i.e.*, $E_{Zeeman} \ll kT$) approximation is caused by time modulation of the quadratic zero field splitting (zfs) interaction [8], arising from Brownian motions of the paramagnetic complex (*e.g.* $Mn[H_2O]_6^{2+}$) and/or from collisions between solvated ions and solvent molecules [9]. On the basis of the assumption of a negligible hyperfine interaction, Redfield's relaxation matrix can easily be calculated (*cf.* [7]). As was previously shown [7], corrections due to time-fluctuating second-order effects caused by cross products of the electron and nuclear spin operators [10] are negligibly small for correlation times τ smaller than about 50 ps. The relaxation rates, $1/T_2$, for the 30 allowed electron transitions ($\Delta M = \pm 1$, $\Delta m = 0$; where M and m are the magnetic electron and nuclear spin quantum numbers) are given by the eigenvalues of the following relaxation matrix:

$$R = -\frac{\Delta^2}{10}\begin{pmatrix} A & D & E & 0 & 0 \\ D & B & 0 & F & 0 \\ E & 0 & C & 0 & E \\ 0 & F & 0 & B & D \\ 0 & 0 & E & D & A \end{pmatrix} \qquad (1a)$$

with

$$\begin{aligned} A &= 24J_0 + 48J_1 + 28J_2 & D &= -8\sqrt{10}\cdot J_1 \\ B &= 6J_0 + 36J_1 + 46J_2 & E &= -12\sqrt{5}\cdot J_2 \\ C &= 16J_1 + 56J_2 & F &= -36\cdot J_2 \end{aligned} \qquad (1b)$$

where the spectral density J_k is defined as:

$$J_k = 2\tau/(1 + k^2\,\omega_0^2\cdot\tau^2)\,. \qquad (1c)$$

The relative intensities are related to the corresponding eigenvectors of Eqn (1a). The symbols in Eqns (1a–c) have the following meaning: Δ^2 is the trace of the squared zfs-tensor which is chosen to be diagonalized in the molecular fixed frame, $\Delta^2 = {}^2/_3\,D^2 + 2E^2$, where D and E are the axial and rhombic distortion parameters of the time-modulated zfs-interaction; the correlation time τ describes this time modulation on a microscopic time scale; ω_0 is the Larmor frequency. In Fig. 2 the three relaxation rates for the corresponding electron transitions are shown as a function of the correlation time τ and correspondingly the relative intensities are represented in Fig. 3. The line position of the 30 transitions can be calculated to the fourth order in perturbation from the static Hamiltonian [11]

$$\hat{H}^0 = \beta\cdot g\cdot H_{0z}\cdot\hat{S}_z + A\cdot\hat{S}\cdot\hat{I} \qquad (2)$$

where β is Bohr's magneton; g is the g-factor; H_{0z} is the z-component of the magnetic field strength, and A is the hyperfine coupling constant between the electron and nuclear spin which are symbolized by their corresponding operators $\hat{S}$, $\hat{I}$. Provided that, $T_2 \gg \tau$, each line is given by a Lorentzian with a half width of $2/T_2$. Using Eqns (1, 2) spectra simulation therefore is a straightforward process. The unknown properties in Eqns (1, 2) are: Δ, τ, and A. For A a value of 9.4 millitesla (mT) has been found to give the best fit of the total line width between simulated and measured spectra.

RESULTS AND DISCUSSION

Measurements at two different frequencies make possible the determination of Δ and τ from a comparison of the calculated and measured spectra. In Fig. 4 and 5 this procedure has been demonstrated. In Fig. 4, the X-band spectrum (full line) of a concanavalin A sample containing only Mn^{2+} ions (at 4 °C) is shown and correspondingly in Fig. 5 the Q-band spectrum (full line) is represented. The dotted curves in Fig. 4 and 5 are calculated spectra with a correlation time $\tau = (10 \pm 1)$ ps and a crystal field parameter, $\Delta = (27 \pm 3)$ mT. The corresponding values for an aqueous Mn^{2+} solution at 4 °C are: $\tau = (5.8 \pm 0.5)$ ps and $\Delta = (15 \pm 1.5)$ mT. These values show the relatively high mobility of manganese ions in the polymer protein phase. The higher

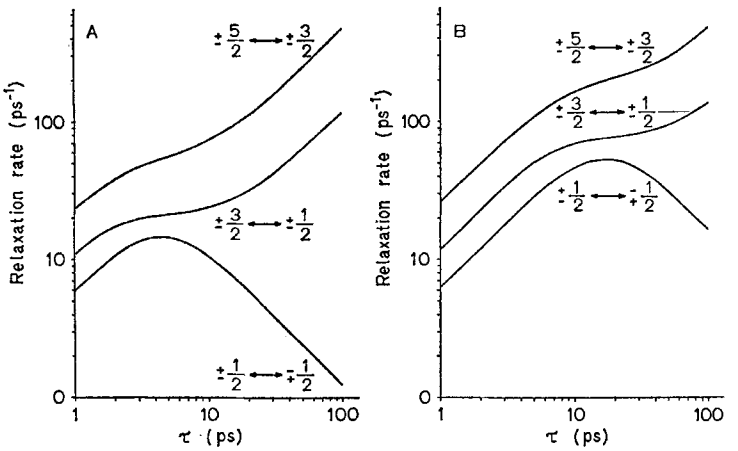

Fig. 2. *Relaxation rates, $1/T_2$ (in units of $\Delta^2 \cdot S$) as a function of the correlation time τ for the various electron transitions of a $S = 5/2$-electron spin system at (A) 35 GHz and (B) 9.5 GHz*

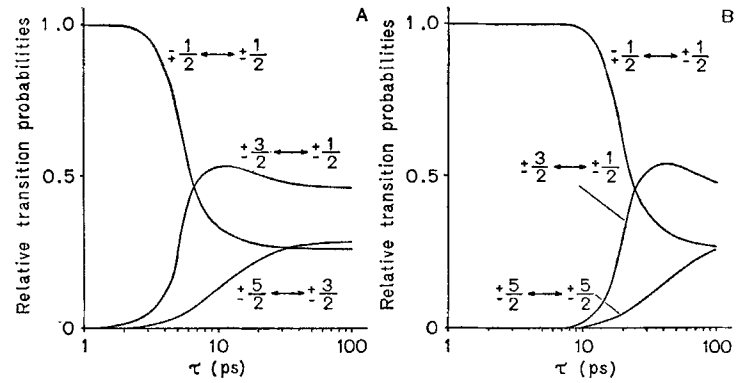

Fig. 3. *Relative transition probabilities as a function of the correlation time τ for the various electron transitions of a $S = 5/2$-electron spin system at (A) 35 GHz and (B) 9.5 GHz*

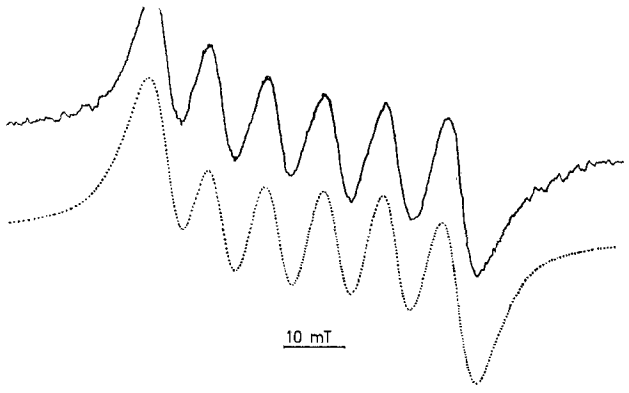

Fig. 4. *Measured (full line) and stimulated (dotted line) EPR-spectra at 9 GHz (shifted base lines). $T = 4$ °C*

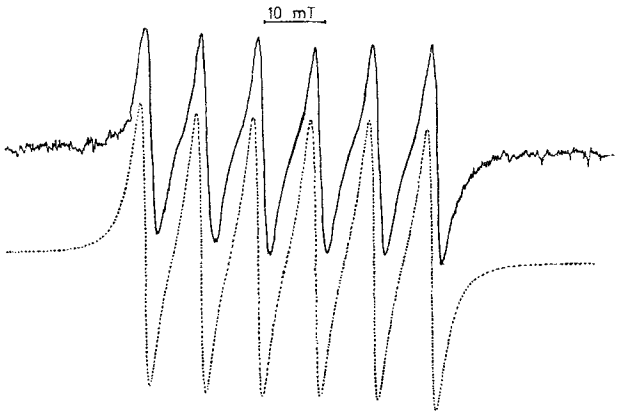

Fig. 5. *Measured (full line) and simulated (dotted line) EPR-spectra at 35 GHz (shifted base lines). $T = 4$ °C*

Table 1. *Correlation time τ and zfs-parameter Δ of Mn^{2+}-concanavalin (without Ca^{2+}) at various temperatures*

T	τ	Δ
°C	ps	mT
4	10 ± 1	
15	7.8 ± 0.8	27 ± 3
25	6.5 ± 0.5	
35	5.3 ± 0.5	

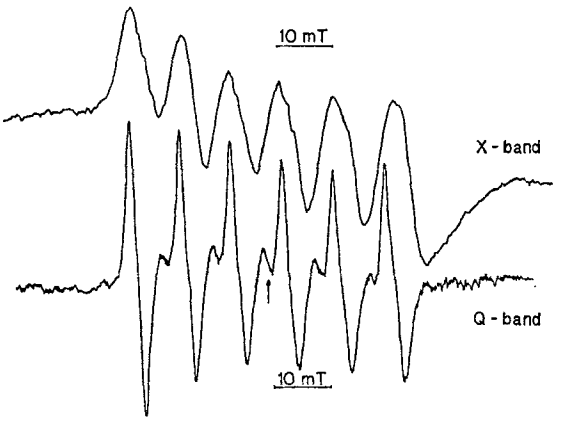

Fig. 6. *Mn^{2+}-EPR spectrum of concanavalin A containing Ca^{2+} ions at 9 GHz (X-band) and 35 GHz (Q-band). T = 4 °C*

values of Δ indicate that the average ligand field around a manganese ion in the protein is more disturbed (from an octrahedral symmetry) than in pure water. Obviously the manganese ions are placed inside the protein phase from where they cannot easily escape, although the protein is still in contact with the bulk water phase. From the results shown in Fig. 1, it follows that the measured spectra (*cf.* Fig. 4 and 5) are mainly due to metal ions "bound" in the protein and that the contributions of manganese ions dissolved in the bulk water phase is negligibly small (about a factor of 10). The temperature dependence of the correlation times between 0 °C and 35 °C is given by an Arrhenius plot with an activation energy of about 3.5 kcal/mol. In Table 1 the values of τ for various temperatures are listed.

At temperatures below 0 °C additional signals appear which are due to so-called forbidden transitions ($\Delta m = \pm 1$). These new lines, located between the main transitions ($\Delta M = \pm 1$, $\Delta m = 0$) are caused by second-order (time-independent) effects due to cross products of the electron and nuclear spin operators [12]. They can always be observed when the ligand field has an axial symmetry and the angle between the crystal axis and the direction of quantization (given by the static magnetic field H_{0z}) is different from zero [12]. As long as the mean lifetime, τ_{ass}, for a molecule fixed vector at a certain angular position relative to the laboratory fixed frame is of the order of picoseconds, which is a typical value for rotational diffusion as it prevails at room temperature, no forbidden transitions are observable.

In Fig. 6, the X-band and Q-band spectra of concanavalin A (at 4 °C) containing both metal ions, namely Mn^{2+} (at S1) and Ca^{2+} (at S2) are shown. Because of the broader line-width at lower frequencies, the forbidden transitions are better resolved at 35 GHz (*cf.* Fig. 6). (At 35 GHz it is still too broad for the $\Delta m = \pm 1$ doublets to be well resolved.) The relative intensity between the $\Delta m = \pm 1$ transitions and the ordinary transitions is given [12] as

$$I_{rel} = \left(\frac{3D \cdot \sin 2\theta}{4g \cdot \beta \cdot H_{0z}}\right)^2 \cdot \left(1 + \frac{S(S+1)}{3M(M-1)}\right)^2 \{I(I+1) - m^2 + m\} \quad (3)$$

where D is the axial distortion parameter, already introduced; β is Bohr's magneton and θ is the angle between the direction or the magnetic field, H_{0z}, and the crystal axis. S, M, I, m are the usual symbols for the electron and nuclear spin quantum numbers. Using the measured relative intensity (an integrated intensity, $h \cdot \Delta H^2$, was used, where h is the peak-to-peak amplitude and ΔH is the peak-to-peak line width) between the fourth line and the corresponding forbidden transition (indicated by an arrow in Fig. 6), the axial distortion parameter D can be calculated. The angle dependence in Eqn (3) was taken as an average over all possible angles: $\overline{\sin 2\theta} = {}^1/_2$. A value of 7.0 mT was found for D. This value of D indicates a weak axial symmetry for manganese ions located in concanavalin A at S1 positions. Since the value of I_{rel} does not change with decreasing temperatures (−40 °C), we can state that all transition metal ions occupy the S1 positions (at 4 °C). (For 25 °C the same value of I_{rel} has been found.) This behavior is in contrast to that of manganese ions "bound" in simpler polymers, such as sulfonated polystyrene cation-exchange resins (*cf.* [7]), and it demonstrates the high affinity of the binding sites S1 which is lost in the absence of Ca^{2+} ions located at S2 (*cf.* Fig. 4 and 5). The value of D corresponds more closely to those found for inorganic crystals [13] like $Mn(NO_3)_2 \cdot 2Bi(NO_3)_2 \cdot 24\,H_2O$ (with D = 7.7 mT) containing much water rather than to strongly axial symmetric systems, such as Mn^{2+} in a sulfonated polystyrene matrix [7] (with D = 15 mT). At the present moment, however, we do not know whether this value supports the model proposed by Kalb and coworkers [14, 15] with two imidazol groups from two histidine molecules as ligands or the model proposed by Edelman and coworkers [16] with only one histidine, one glutamic, and two aspartic acid ligands. Further investigations are necessary (in particular the determination of E the rhombic distortion parameter) in order to decide which ligands are more likely. Such a study is in preparation.

Substitution of Ca^{2+} ions by Mg^{2+} or Ba^{2+} yields a manganese spectrum similar to that of Ca^{2+}/Mn^{2+}-concanavalin A, *i.e.* $\Delta m = \pm 1$ transitions can be observed. However, the intensity (measured in a double cavity) of the Mn^{2+} spectrum is smaller (by about a factor of 5) compared to the corresponding Ca^{2+}/Mn^{2+}-concanavalin A spectrum. We therefore conclude that because of the somewhat different ionic radii of Mg^{2+} and Ba^{2+} their structure stabilizing ability is diminished resulting in a reduction of the affinity of S1 binding sites for Mn^{2+} ions.

Since the $\Delta m = \pm 1$ transitions at a frequency of 9 GHz are not very well resolved, they have not been identified in a previous study of concanavalin A dissolved in an aqueous solution [17]. Therefore we also measured the EPR spectrum at 35 GHz of Ca^{2+}/Mn^{2+}-concanavalin A dissolved in an aqueous 4 M NaCl solution. The spectrum was found to be almost identical to that shown in Fig. 6 (lower curve). And again a value of about 7 mT for the axial crystal field parameter D has been determined. The moderate increase of the intensity and the narrowing of the individual absorption lines, observed for the X-band spectrum when $CaCl_2$ was added either before or after $MnCl_2$ to an aqueous solution of demetallized concanavalin A, as described by Kalb and coworkers [17] therefore can be attributed to $\Delta m = \pm 1$ transitions which are not resolved at 9 GHz.

CONCLUSIONS

Summarizing we can confirm that both the transition and the calcium ions are necessary (cooperative process) to create a certain specific structure of concanavalin A. The mean life-time of Mn^{2+} ions at the binding sites S1 in the absence of Ca^{2+} ions is determined by the thermal motions of the diffusing metal ions, but becomes considerably longer when Ca^{2+} occupies the S2 positions. The structure-stabilizing effect of Mg^{2+} or Ba^{2+} with their different ionic radii compared to Ca^{2+} seems to be reduced which indicates the relatively high stereo-specifity of the S2 binding sites.

We are greatly indebted to Prof. Dr A. Müller-Broich for helpful discussions.

REFERENCES

1. Sumner, J. B. & Howell, S. F. (1936) *J. Biol. Chem. 115*, 583–588.
2. Sumner, J. B. & Howell, S. F. (1936) *J. Bacteriol. 32*, 227–237.
3. Goldstein, I. J., Hollerman, C. E. & Merrick, J. M. (1965) *Biochim. Biophys. Acta, 97*, 68–76.
4. Inbar, M. & Sachs, L. (1969) *Proc. Natl. Acad. Sci. U. S. A. 63*, 1418–1425.
5. Kalb, A. J. & Lustig, A. (1968) *Biochim. Biophys. Acta, 168*, 366–367.
6. Kalb, A. J. & Levitzki, A. (1968) *Biochem. J. 109*, 669–672.
7. Goldammer, E. v., Müller, A. & Conway, B. E. (1974) *Ber. Bunsenges. Phys. Chem. 78*, 35–42.
8a. McGarvey, B. R. (1957) *J. Phys. Chem. 61*, 1232–1237.
8b. Bloembergen, N. & Morgan, L. O. (1961) *J. Chem. Phys. 34*, 842–850.
9. Rubinstein, M., Baram, A. & Luz, Z. (1971) *Mol. Phys. 20*, 67–80.
10. Luckhurst, G. R. & Pedulli, G. F. (1970) *Chem. Phys. Lett. 7*, 49–52.
11. Hurd, F. K., Sachs, M. & Hershberger, W. D. (1954) *Phys. Rev. 93*, 373–380.
12. Bleaney, B. & Rubins, R. S. (1961) *Proc. R. Soc. Lond. B, Biol. Sci. 77*, 103–112.
13. Ingram, D. J. E. (1953) *Phys. Rev. 90*, 711.
14. Weinzierl, J. & Kalb, A. J. (1971) *FEBS Lett. 18*, 268–270.
15. Gachelin, G., Goldstein, L., Hofnung, D. & Kalb, A. J. (1972) *Eur. J. Biochem. 30*, 155–162.
16. Edelman, G. M., Cunningham, B. A., Reeke, G. N., Jr, Becker, J. W., Waxdal, M. J. & Wang, J. L. (1972) *Proc. Natl. Acad. Sci. U. S. A., 69*, 2580–2584.
17. Nicolau, C., Kalb, A. J. & Yariv, J. (1969) *Biochim. Biophys. Acta, 194*, 71–73.

E. von Goldammer and H. Zorn, Lehrstuhl für Physik, Fachbereich Biologie der Universität Regensburg, D-8400 Regensburg 2, Universitätsstraße 31, Federal Republic of Germany